High Precision Humidity Controller - Design Proposal and Validation

Author:

B. Sejdijaj,

Supervisors:

Prof. Dr. Ir. J.E. ten Elshof, Ing. K.J.H. van den Nieuwenhuijzen and Dr. J. A. Alvarez-Chavez

University of Twente
Inorganic Materials Science Group

April, 2019

Contents

1 General

Electro spinning is fiber production method where ultra thin fibers are created from polymer solutions using large electric forces. The most general approach is to generate a large electric potential between a syringe containing some polymer solution and large collector plate. As the substance leaves the syringe, that material is elongated and pulled towards the collector plate. In literature, multiple approaches exist to achieve similar goals [1].

Despite the apparent simplicity of the electro spinning principle, the process itself is quite complicated because many parameters influence the properties of the obtained nanofibrous structures. These parameters can be merged in three groups, solution parameters, processing parameters and ambient parameters. Most of the research work published so far has focused on parameters belonging to the first two groups. However, ambient parameters such as humidity, temperature and ambient gas composition influence the process and the outcome of the process[2].

Previous work has shown that temperature and RH are two ambient parameters that strongly affect electro spinning. RH makes the thicker or thinner, depending on the chemical nature of the polymer. The change in temperature causes two main and opposing effects to change the average diameter. Evaporation rate of the solvent and viscosity of the solution are two opposing mechanism that have an effect on the mean fiber diameter [2], [3].

In this manual, an approach towards controlling for these parameters is presented. This performance of this approach will be theoretically approach and an hardware implementation will be presented to illustrate the expected real world performance.

2 Working Principle

The relative humidity that we want to control is described by ration between the partial pressure of vapor over the saturated partial pressure of that gas $\frac{P_{H_2O}}{P_{H_2Os}}$[4]. However, controlling this accurately is very challenging. For control purposes of the experiment tank in question, it is more convenient to control the specific humidity, which is described as the ratio of the mass of water vapor to the total mass of the moist air parcel. The mixing ratio is much easier to control as mass flow can more accurately be measured and controlled than partial pressures in a mixed gas.

2.1 Relating Relative And Specific Humidity

A relation between the specific and relative humidity needs to be established in order to control one with the other. Starting from the definition of specific humidity, which is the mass mixing ratio of water vapor in air, defined as:[4]

$$q \equiv \frac{m_v}{m_v + m_d} = \frac{\omega}{\omega + 1} \approx \omega \tag{1}$$

where m_v is the specific mass of water vapor [kg], m_d is the specific mass of dry air [kg], ω is the mass mixing ratio of water vapor to dry air [%] and q is the specific humidity or the mass mixing ratio of water vapor to total air [%]. We can say that the specific humidity q is approximately equal to the mass mixing ratio ω.

Relative humidity can be expressed as the ratio of water vapor mixing ratio to saturation water vapor mixing ratio $RH = 100\frac{\omega}{\omega_s}$, where:

$$\omega_s \equiv \frac{m_{vs}}{m_d} = \frac{R_d}{R_v}\frac{e_s}{P - e_s} \approx 0.622\frac{e_s}{P} \tag{2}$$

where ω_s is the mass mixing ratio of water vapor to dry air at equilibrium [%], m_{vs} is the specific mass of water vapor at equilibrium, e_s saturation vapor pressure [Pa], R_d and R_v are the specific gas constant for dry air and vapor [$Jkg^{-1}K^{-1}$] and the pressure in the experiment P [Pa].

In this expression, the saturation vapor pressure e_s can be described by the Clausius–Clapeyron relation:[5]

$$e_s(T) = e_{s_0}\exp[\frac{L_v(T)}{R_v}(\frac{1}{T_0} - \frac{1}{T})] \approx 611\exp[\frac{17.67(T - T_0)}{T - 29.65}] \tag{3}$$

where L_v is the specific enthalpy of vaporization [Jkg^{-1}] and T_0 is the reference temperature 273.15 K. Since ω and ω_s are know, the RH can now be described in terms of specific humidity q. The final expressions thus become:

$$RH = 100\frac{\omega}{\omega_s} = 0.263P_0q[\exp[\frac{17.67(T - T_0)}{T - 29.65}]]^{-1} \tag{4}$$

$$q = \frac{3.80\ RH}{P}\ \exp[\frac{17.67(T - T_0)}{T - 29.65}] \tag{5}$$

2.2 Theoretical Model

With the knowledge that the mixing ratio can be used to approximate the RH, the design of a simple humidity controller becomes trivial. The approach that will be used for the design of the humidifier will be to very precisely mix dry air with vapor and blow this into the experiment tank. The desired mixing ratio is calculated using the relations found in the previous section. The practical (real world) approach towards making this idea viable, is to use a controlled evaporator mixer like Bronkhorst's W-300B along with mass flow controllers to very precisely mix the dry air and water. This mixture is than blown into an experiment tank, which will subsequently cause the air inside of the tank to be blown out.

The air in the experiment tank can no be modeled as a mixing problem. Since the gas flows at very low velocities (M < 0.1), it can be considered to be an incompressible fluid. This implies that under steady state, the volumetric flow rate of the inflowing air will be equal to that of the outgoing air[6]. The gas composition in the experiment tank will be controlled by a fixed inflow of mass of the desired composition q_in, the resulting outflow will be of composed of q_tank which is the mass ratio of the gas mixture that is currently present in the tank.

The mass is described in terms of components m_v and m_d, which respectively are the vaporized water and dry air present in the tank.

$$\frac{dm_v}{dt} = \frac{dm_{in}}{dt}\ q_{in} - \frac{dm_{out}(q_{tank}(t))}{dt}\ q_{tank} \tag{6}$$

$$\frac{dm_d}{dt} = \frac{dm_{in}}{dt}\ (1 - q_{in}) - \frac{dm_{out}(q_{tank}(t))}{dt}\ (1 - q_{tank}) \tag{7}$$

Solving this system of differential equations over time will allow us to find the specific humidity $q_{tank}(t) = \frac{m_v(t)}{m_d(t)+m_v(t)}$. The mass inflow is a fixed value, the outflow rate however needs

to be determined. This outflow rate is a function of q because change in humidity subsequently changes the density of the gas and thus the volumetric flow rate. In order for this outlet mass flow rate to be determined, the total volumetric flow rate can be divided by the density ρ of the air inside of the tank. This density is a determined by the mixture of air and water, and is described in equation 9.

$$\frac{dm_{out}(q_{tank}(t))}{dt} = \frac{\dot{V}_{in}}{\rho(q_{tank})} \tag{8}$$

$$\rho(q_{tank}) = \frac{P_0}{R_{air}(q_{tank})T} \tag{9}$$

$$R_{air}(q_{tank}) = \frac{R}{(\frac{q_{tank}}{M_{H_2O}} + \frac{1-q_{tank}}{M_{dryair}})^{-1}} \tag{10}$$

As figure 2 shows, the density correction performed in equation 9 is important to ensure accuracy is maintained over the whole range of user scenarios. Under typical room temperature scenarios however, this effect seem to be modest. As soon as temperatures over 35 ^oC are considered, this correction becomes significant. The correction utilized here is however limited in inaccuracy as it still rely on the conversion from RH to q in equation 5.

2.3 Numerical Approximation And Discussion

Using this theoretical model, the specific humidity can be described by solving equation 6 and 7 simultaneously, the resulting function $q_{tank}(t)$ is found. Because of the complexity of these equations, they were solved numerically, its results are presented in figure 3c.

In the numerical experiments, two transitions were considered. One from 40% to 50%, and one from 30% to 50% RH, these RHs were chosen to illustrate typical user scenarios, while also being a good indicator for nominal resource usage under room temperatures. Additionally, three mass flow rates within the expected operational range were chosen to illustrate nominal performance metrics. The desired q_{in} was determined using equation 5. As boundary conditions, the pressure and temperature were assumed to be a nominal $101350Pa$ and $293.15K$ and the tank volume was assumed to be 10 L.

The first aspect that is interesting to observe is that the settling time seems to only be determined by the total mass flow rate and is independent of the final set point. Implying that the only action required to achieve a particular performance metric, is to tune the total inflow rate. Additionally, the required resources for an experiment are dependent on the desired RH. In this experiment the desired humidity was set at a nominal 50%, The settling time at $1g/s$ is estimated to be 30-40 seconds. In order to achieve this, *60 ml of water and 0.4 kg of dry air* is required for a 10L tank. These values will skew differently for different desired humidities and tank sizes, but from this experiment, the expected settling time will be in the magnitude of minutes.

This numerical experiment is a good pointer towards the expected performance of a practical implementation of such a system. This performance was designed with a relatively simple control scheme. The desired humidity is continuously blown into the tank. The performance of the humidifier can be greatly enhanced by for example increasing the initial mass flow rate and decreasing it as the goal is approached. Another way to improve settling time is to initially use a high vapor flow rate and decrease this as the goal is reached. The topic of advanced control is outside of the scope of this theoretical validation, but further research could be done into this in order to enhance settling times.

2.4 Model Uncertainty

The largest glaring issue with the presented control schemes is however that its a blind method that relies on the accuracy of the theoretical model. Any inaccuracy in the model translates into a direct inaccuracies in the tank humidity. In the presented model, this uncertainty does not only exist in the form variable uncertainty.

Three main major simplifications were performed during the derivation. The first one is equation (1) in which the relation between specific humidity $q = \frac{m_v}{m_d+m_v}$ and the mass mix ratio $\omega = \frac{m_v}{m_d}$ is discussed. Here the simplification $\frac{\omega}{\omega+1} \approx \omega$ is introduced in order to find a direct relation between these two variables. The underlying assumption being that omega is sufficiently small to be neglected in the denominator. Under normal and room temperature, a good case for this can be made. The saturation specific humidity at normal temperatures is in the neighborhood of 10 g/kg as can be found from the Clausius-Clapeyron relations in figure 1. The resulting error of e_ω can be described by

$$e_\omega = \frac{|\frac{\omega}{\omega+1} - \omega|}{\frac{\omega}{\omega+1}} = 1 - \frac{\omega+1}{1} = \omega \tag{11}$$

The error is linearly related to the magnitude of ω. Under normal temperatures and operating conditions, this won't be higher 1 %. However, as temperatures increase the saturation specific humidity increases exponentially. To illustrate this, a RH of 50% at room temperature will result in an $e_\omega < 0.5\%$, while the same RH at 40 ^oC will result in an uncertainty of $e_\omega \approx 2.5\%$. This uncertainty exponentially increases as a function of temperature when other variables are controlled.

The second uncertainty is the model used to approach the saturation pressure in equation (3). This is one of many such models that are related to the Clausius-Clapeyron relations. In order to find the uncertainty of this model, it was compared to empirical test data [8], see figure 4. This show that the accuracy at low temperatures is very good and consistently sits below 0.2%. However, after the 35 ^oC mark the error increases exponentially. At around 65 ^oC, the model surpasses the 1 % error mark and continues rising steadily.

The last source of model uncertainty is the simplification $\frac{e_s}{P-e_s} \approx \frac{e_s}{P}$ in equation (2). The underlying idea here is similar to the first one. e_s assumed to be sufficiently small to be neglected. The total error is described by e_{e_s}:

$$e_{e_s} = \frac{|\frac{e_s}{P-e_s} - \frac{e_s}{P}|}{\frac{e_s}{P-e_s}} = \frac{P}{P} - \frac{P-e_s}{P} = \frac{e_s}{P} \tag{12}$$

Under normal conditions P = 101325 Pa and using the same empirical data [8] to analyze the error, the results from figure 5 can be observed. The uncertainty created by this simplification is major due to the exponential increase with temperature of the saturation pressure. Even at room temperature the error is estimated to be 2% and over 6% at 40 ^oC.

To conclude, the model as presented in this chapter suffers from several major simplifications that make the model suited for a limited area of application. The model seems to only be suited to find mass mix ratios under room temperature or lower, this is because the total error of the model increases exponentially with temperature. Additionally, the model should also be used for small mix ratios in the order of 10 g/kg. Larger mix ratios will cause increases in the model uncertainty. This, again, is especially relevant at higher temperatures. The recommended area of application of this model is at room temperature and below.

While the model performance discussed in this section is sufficient for the goal of estimating system performance, future implementations (especially if higher temperatures are desired)

will require higher fidelity models. Simplifications in equation (1) and (3) should be avoided and a higher accuracy saturation pressure model like for example The Buck equation should be considered.

3 Hardware

In this section the hardware implementation of the humidity controller will be discussed. First an overview will be provided after which the individual components will be covered. This is intended to clarify the realization of a real implementation discussed in section 2 as well as uncover its limitations.

3.1 Overview

Figure 6 is a schematic overview of the hardware implementation of the humidifier. This system design is centered around the central evaporator unit, which is the main mixing device that is able to control both the temperature and mass mixture ratio. It has two inlets which allow a gas and a liquid of choice to be mixed. This evaporator controller is connected electrically to liquid flow controller as this is the main negotiator between the two flows. It controls the mixing valve inside of the evaporator head as can be seen in figure 7. Both inlets are connected to their dedicated mass flow meter/controller. These units do as their name implies, measure and control the mass flow into the evaporator unit. The Airflow controller can do this with its own dedicated valve, while the liquid controller utilizes the mixing valve in the evaporator unit[9].

The process is driven passively by a compressed dry air tank which has a typical pressure of about 200 bar[10], which valve 1 should step down to something in the range of about 10 bar. This pressure will be used to drive the gas through the airflow controller and into the experiment tank. Additionally, the pressure from the compressed air will also to drive the liquid into the fluid flow controller. Protection and bleed valves 2, 3 and 4 are added to allow the water tank to be depressurized and maintained. Similarly valve 5 and 6 allow the experiment tank to be depressurized and the evaporator to be maintained.

The air in the dry air tank is provided by Linde gas and is synthetic mixture of 20% oxygen and 80% nitrogen. As their data sheet indicates, this mixture has a typical filling of about of about 200 bar at 15 degrees C. The purity of the gas is guaranteed to be at least 99.5% depending on what is ordered. In the cheapest variant, the impurity of H_2O is said to be smaller than 67 ppm all the way up to 0.5 ppm[10].

The water in the water reservoir should be distilled H_2O. This is in order to prevent impurities from damaging the internal tubing and other devices. The tank should have a high rating to withstand the pressure that the compressed air will apply onto it.

In order to provide closed loop control capabilities one or multiple humidity can be integrated into the experiment setup. These sensors are connected through a I2C digital data bus which theoretically allows for up to 127 devices to be connected on one bus[11].

3.2 Controlled Evaporator

In this hardware implementation, the controlled evaporator mixer W300-B from Bronkhorst will used to control the mixing of the gas. This device has a capacity to mix up to 1200 g/h which comes down to about 330 mg/s and a maximum gasflow of up to $100 l_n/min$ (l_n being

nominal gas at 0 ^oC and 101kPa), which comes down to about 2.15 g/s of gas. This is a large bottleneck with respect to the desired 8 - 15 g/s as discussed in section 2. The maximum operating pressure is rated to be about 100 bar[9].

The main mixing valve inside of the evaporator controls the rate at which water and air are mixed and is steered by the liquid flow controller. The mixed gas will then be lead into the heated section where the mixture will be evaporated. The unit allows the mixture to be heated all the way to 200 ^oC, this capability is what allows for the temperature in the experiment tank to be controlled alongside the humidity. Note however that dynamically changing the temperature will result in require the theoretical model from section 2 to be expanded to accommodate for this. Changing the temperature changes the saturation specific humidity significantly (as shown in figure 1) which will lead to higher mass ratios to be achieved, for a certain RH.

3.3 Fluid Mass Flow Meter

mini CORI-FLOW ML120 instruments by Bronkhorst® are precise and compact Mass Flow Meters and Controllers for liquids and gases, based on the Coriolis measuring principle. Designed to cover the needs of the (ultra) low flow market, from 5 g/h up to 200 g/h (full scale values), the mini CORI-FLOW offers multi-range functionality: factory calibrated ranges can be rescaled by the user, maintaining the original accuracy specifications. This results in a maximum liquid flow of about 56 mg/s [12].

Instruments of the mini CORI-FLOW series contain a uniquely shaped, single loop sensor tube, forming part of an oscillating system. When a fluid flows through the tube, Coriolis forces cause a variable phase shift, which is detected by sensors and fed into the integrally mounted printed circuit board. The resulting output signal is strictly proportional to the real mass flow rate. Coriolis mass flow measurement is fast, accurate and inherently bi-directional. The mini CORI-FLOW features density and temperature of the fluid as secondary outputs[12].

A Coriolis flow meter contains a tube which is energized by a fixed vibration. When a fluid (gas or liquid) passes through this tube the mass flow momentum will cause a change in the tube vibration, the tube will twist resulting in a phase shift. This phase shift can be measured and a linear output derived proportional to flow. As this principle measures mass flow independent of what is within the tube, it can be directly applied to any fluid flowing through it whereas thermal mass flow meters are dependent of the physical properties of the fluid. Furthermore, in parallel with the phase shift in frequency between inlet and outlet, it is also possible to measure the actual change in natural frequency. This change in frequency is in direct proportion to the density of the fluid – and a further signal output can be derived. Having measured both the mass flow rate and the density it is possible to derive the volume flow rate[13], [14].

The accuracy of a mini CORI-FLOW is either 0.2% reading for liquids or 0.5% reading for gases. This specification is based on mass flow (e.g. g/h, kg/h, etc.). Using the instrument for measuring volume flows (e.g. l/h, ml/min) will introduce an additional inaccuracy, based on the actual density measured by the instrument. In all instruments capable of density measurement there will be an automatic adjustment for change in density[12].

3.4 Gas Mass Flow Meter

The gas measurements and control are performed by the EL-Flow Select by Bronkhorst® which is high accuracy mass flow measurement and control device for fluids. The instrument is

equipped with a piezoelectric valve that can restrict the fluid flow, this valve is controlled by itself. The user has the ability to write a certain set point and the internal PID controller will set the valve to an appropriate position for the desired mass flow. This system is rated for a maximum pressure of 100 bar and a mass flow rate of up to 250 l_n/min (l_n being nominal gas at 0 ^oC and 101kPa), which equates to a mass flow of about 5.4 g/s[15].

The measurement principle used to determine the mass flow uses an in-line heating element with two equidistant temperature sensors as is visible in figure 9. The approach is to provide a constant input power to a section of tubing and measure the temperature of the tube on both sides of the heated section. The flowing gas skews the temperature such that the downstream temperature is larger than the upstream value. This measured difference is linearly dependent upon mass flow to first order according to[16]

$$\dot{m} = \frac{Q}{C_p(T)(T_2 - T_1)} \tag{13}$$

where $C_p(T)$ is the temperature dependent molar heat capacity $[Jmol^{-1}K^{-1}]$, Q is the rate of heat transfer from the capillary wall to the gas $[J]$, T_2 is the gas temperature downstream of the heated capillary $[K]$, T_1 is the gas temperature upstream of the heated capillary, and $\dot{m}$ is the molar flow $[mols^{-1}]$. This has the convenient property of providing near linear measurement results in a large set of ranges.

3.5 Closing Note

The above section described the hardware implementation for humidity control. A variety of Bronkhorst® instruments were used to try and fulfill the performance requirements, from the analysis as provided above it is to be found the largest bottleneck lies in the controlled evaporator which has a limited capacity of 2.15 grams per second. Running the same numerical simulation as discussed in section 2 on a 10L experiment tank, results in a settling time of about 30 seconds. The issue here however, is that the volumetric flow rate at maximum capacity is about $100l_n/min$. Considering the tubing has a diameter of 6 millimeter, this results in a flow velocity of roughly $15m/s$ under normal conditions (P is 101325, T is 273.15K). The resulting Reynolds number in the tubing will be 5700 using[6]:

$$Re = \frac{\rho_{air} v \ d_{tube}}{\mu} \tag{14}$$

where ρ_{air} is the density at normal conditions $[kg/m^3]$ (1.29 kg/m^3), v is the flow velocity $[m/s]$, d_{tube} is the tube diameter $[m]$ (0.006 m) and μ dynamic viscosity for air [Pa s] (1.98310^{-5} Pa s). This Reynolds number indicates turbulent flow which might disturb the experiment. To ensure laminar flow, designing for a maximum Reynolds number of 2000 yields a maximum flow velocity of about 5 m/s. The subsequent volumetric flow rate is 34 l_n/min or 0.72 g/s. Under these circumstances, the numerical simulation results in a settling time of about 90 seconds, as can be seen in figure 10.

Another factor to consider is the minimum performance, these are dictated by the mass flow meter. The lowest limit of the gas mass flow meter is 0.8 l_n/min which converts to 0.0172 g/s under normal conditions. Additionally, the lowest limit of the vapor mass flow meter is 5 g/h which converts to about 0.00139 g/s. With both machines working at their absolute minimum, a specific humidity of 80 g/kg is to be expected, which under room temperature is fully saturated as can be seen in figure 1.

In order to achieve a typical 50% RH under minimum flow conditions in a laboratory environment (101325 Pa and 293.15K), a specific humidity of 7.2 g/kg is required. Under these circumstances the humidifier is bottlenecked by the limits of the liquid flow meter. The minimum mass flow possible to fulfill the humidity requirement is 0.19 g/s. Similarly, when the requirement is 20% RH at laboratory conditions the minimum mass flow is 0.47 g/s, and for 80% it is 0.12 g/s. The full expected operational area of the humidifier in accordance with the instrument specifications is shown in figure 11. The upper limit is given by the laminar flow limit and any total mass flow beyond this might result in

3.6 Settling Performance

In this section the expected settling performance will be discussed. The settling performance is an indication of the theoretical limit of this hardware implementation. This estimation will assume that the limitations of the model as presented in section 2 are overcome, and an accurate mass mixing ratio can be obtained. the two limiting factors to be considered are the two mass flow meters.

From the calibration report of the mini CORI-FLOW liquid flow meter, we find that its rated accuracy is $\pm 0.2\%$. This accuracy is guaranteed within its operational area 5 g/h and 200 g/h. However, the device calibration indicates that an accuracy of $\pm 0.02\%$ can be obtained in an operational area of 1 g/h up to 200 g/h[12]. The latter will be considered the optimal performance capacity of this measuring instrument. The EL-FLOW Select boasts a rated accuracy of $\pm 0.5\%$ in its operational range of 20 l_n/min to 100 l_n/min. The device was calibrated on dry air and has a measured deviation of $\pm 0.05\%$[15].

Outside of this operational range, the rated accuracy drops significantly to up to 3%. This range will not be considered for the estimation and using the humidifier in this operational area (as indicated by figure 11) is not recommended.

Additionally, the dry air used will have some impurities to be considered. The gas provided by Linde Gas is rated for ≤ 5 ppm of H_2O. At 1 bar and 273.15, this converts to an absolute humidity of 4 mg/m^3 or a specific humidity 3.3 mg/kg. This is being at least a factor 1000 removed from any typical saturation specific humidity at any temperature, this can be neglected entirely[10].

Using these figures, the humidifier can expect a rated accuracy of 0.7% in its operational range., assuming the device calibration is maintained, the best possible performance can be expected to be $\pm 0.07\%$. Considering accurate models, the RH can be controlled with an accuracy of at least $\pm 0.7\%$. When considering current theoretical model's limitations, the accuracy can be expected to be around $\pm 3 - 4\%$ at room temperature.

Bibliography

[1] W. E. Teo and S Ramakrishna, "A review on electrospinning design and nanofibre assemblies", *Nanotechnology*, vol. 17, no. 14, R89–R106, 2006. DOI: 10.1088/0957-4484/17/14/r01. [Online]. Available: https://doi.org/10.1088%2F0957-4484%2F17%2F14%2Fr01.

[2] S. De Vrieze, T. Van Camp, A. Nelvig, B. Hagström, P. Westbroek, and K. De Clerck, "The effect of temperature and humidity on electrospinning", *Journal of Materials Science*, vol. 44, no. 5, pp. 1357–1362, 2009. [Online]. Available: 10.1007/s10853-008-3010-6.

[3] S. Tripatanasuwan, Z. Zhong, and D. H. Reneker, "Effect of evaporation and solidification of the charged jet in electrospinning of poly(ethylene oxide) aqueous solution", *Polymer*, vol. 48, no. 19, pp. 5742 –5746, 2007, ISSN: 0032-3861. DOI: https://doi.org/10.1016/j.polymer.2007.07.045. [Online]. Available: http://www.sciencedirect.com/science/article/pii/S0032386107007185.

[4] A. Wilkes and D. Williams, "Measurement of humidity", *Anaesthesia and Intensive Care Medicine*, vol. 19, no. 4, pp. 198 –201, 2018, ISSN: 1472-0299. DOI: https://doi.org/10.1016/j.mpaic.2018.01.009. [Online]. Available: http://www.sciencedirect.com/science/article/pii/S1472029918300213.

[5] A. L. Young H. D. Freedman R. A. Ford and F. W. Sears, *Sears and Zemansky's University Physics: With Modern Physics.* 13th ed. San Francisco: Pearson Addison Wesley, 2004, ISBN: 0321696861.

[6] G. T. Keith and J. E. A. John, *Gas Dynamics*, 3rd ed. Korea: Pearson Education Korea Ltd., 2016, ISBN: 978-89-450-0178-8.

[7] M. Boukhriss, Z. Khalifa, and R. Ghribi, "Study of thermophysical properties of a solar desalination system using solar energy", *Desalination and Water Treatment*, vol. 51, pp. 1290–1295, Jan. 2013. DOI: 10.1080/19443994.2012.714925.

[8] D. Lide, *CRC Handbook of Chemistry and Physics, 85th Edition*, ser. CRC Handbook of Chemistry and Physics, 85th Ed v. 85. Taylor & Francis, 2004, ISBN: 9780849304859. [Online]. Available: https://books.google.nl/books?id=WDll8hA006AC.

[9] *Instruction manual for controlled evaporator and mixer unit (cem)*, 9.17.126A, Bronkhorst High-Tech B.V., Ruurlo, Netherlands, 2018.

[10] *Gases & applications*, The Linde Group, Pullach, Germany, 2015.

[11] *Um10204 i2c-bus specification and user manual*, v.6, NXP Semiconductors N.V., 2014.

[12] *Instruction manual for mini cori-flow ml120*, 9.17.097G, Bronkhorst High-Tech B.V., Ruurlo, Netherlands, 2018.

[13] J. E. Smith and D. R. Cage, "Parallel path coriolis mass flow rate meter", pat. US4491025A.

[14] J Haneveld, T. S. J. Lammerink, M. J. de Boer, R. G. P. Sanders, A Mehendale, J. C. Lötters, M Dijkstra, and R. J. Wiegerink, "Modeling, design, fabrication and characterization of a micro coriolis mass flow sensor", *Journal of Micromechanics and Microengineering*, vol. 20, no. 12, p. 125 001, 2010. DOI: 10.1088/0960-1317/20/12/125001. [Online]. Available: https://doi.org/10.1088%2F0960-1317%2F20%2F12%2F125001.

[15] *Instruction manual for el-flow select series*, 9.17.099D, Bronkhorst High-Tech B.V., Ruurlo, Netherlands, 2018.

[16] S. A. Tison, "A critical evaluation of thermal mass flow meters", *Journal of Vacuum Science & Technology A*, vol. 14, no. 4, pp. 2582–2591, 1996. DOI: 10.1116/1.579985. [Online]. Available: https://doi.org/10.1116/1.579985.

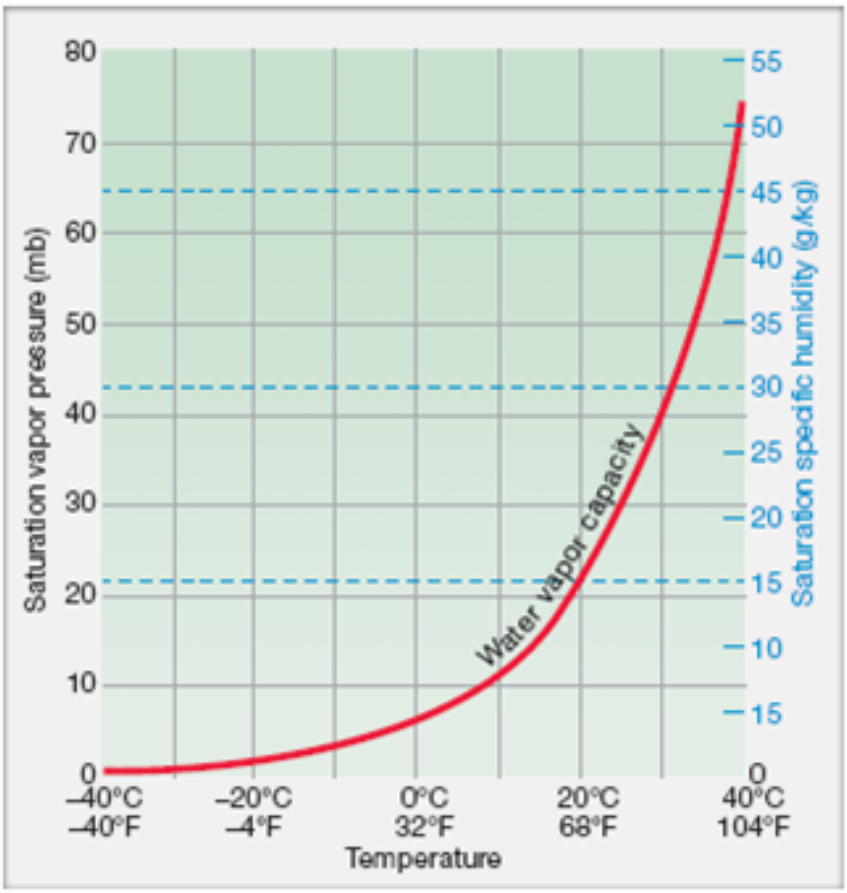

Figure 1: *Saturation specific humidity and temperature graph. This is a solution to the Clausius–Clapeyron relation for water and can be used to find the relative humidity*

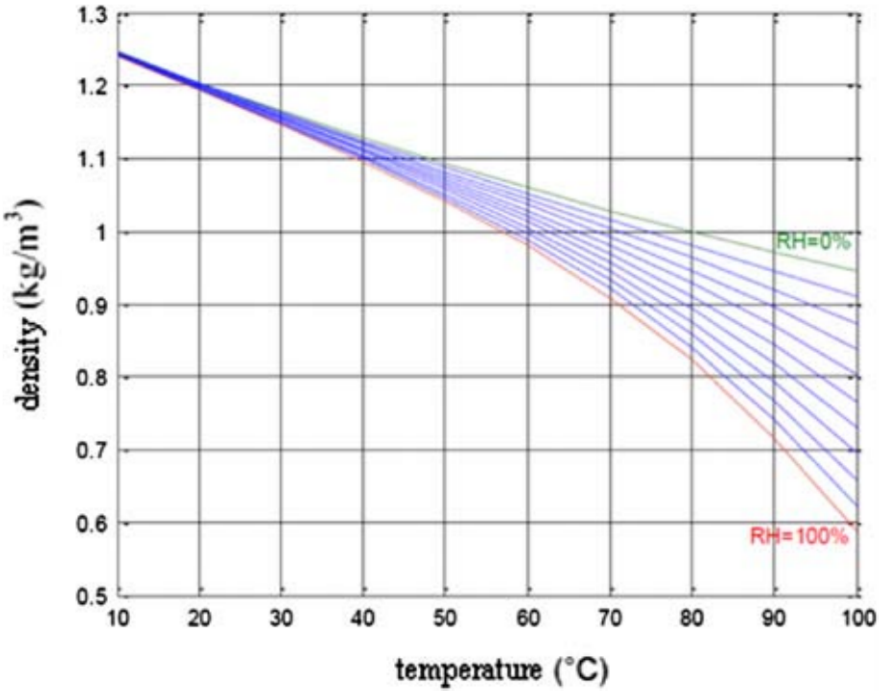

Figure 2: *The relation between air density, temperature and relative humidity[7]*

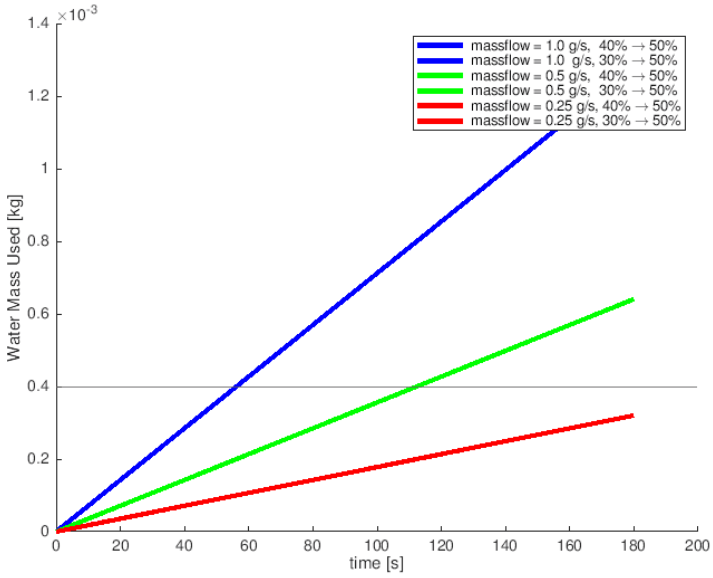

(a) *Simulated results for the used vapor mass as function of time.*

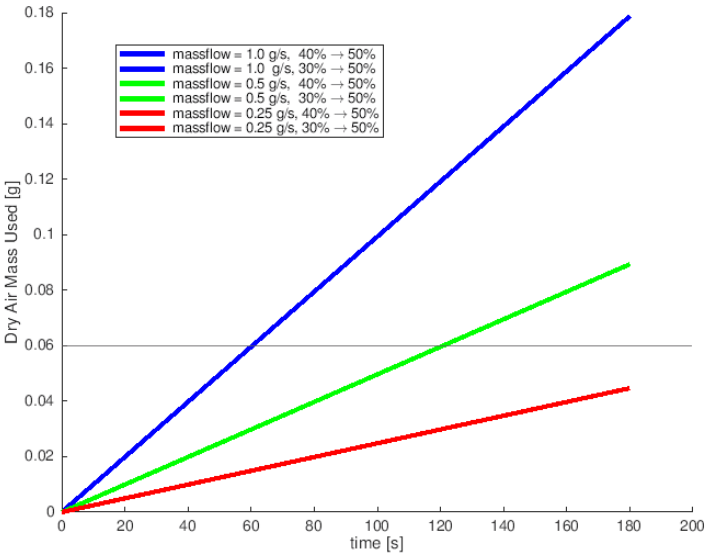

(b) *Simulated results for the used dry air mass as function of time.*

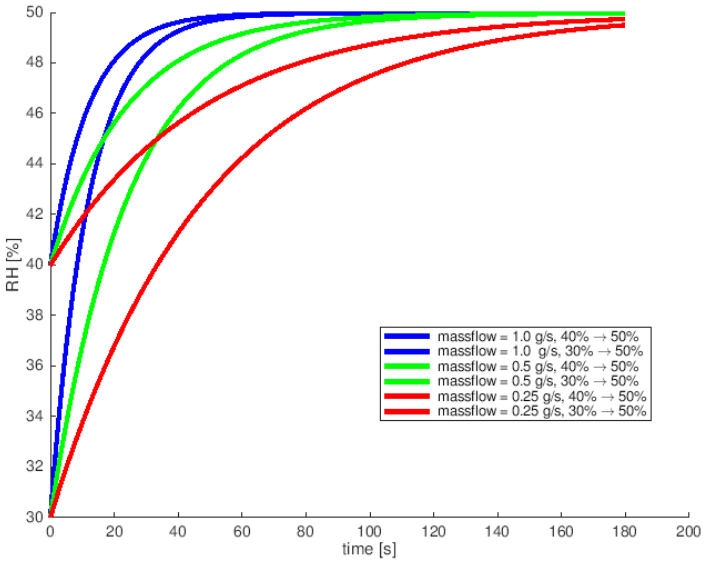

(c) *Simulated results for the RH as a function of time*

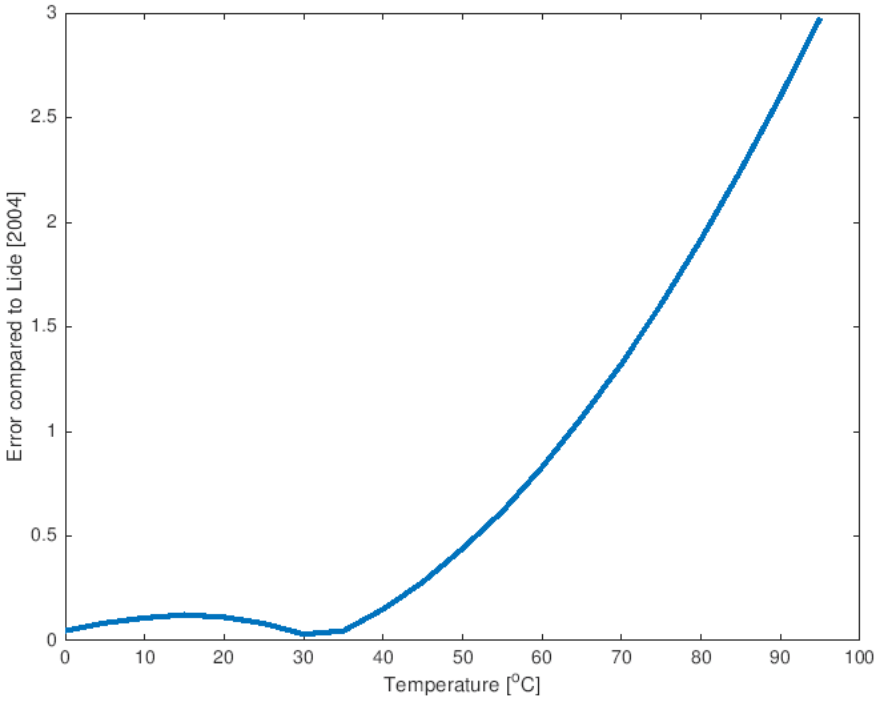

Figure 4: *Model error of the saturation pressure equation (3) tested against empirical data[8]*

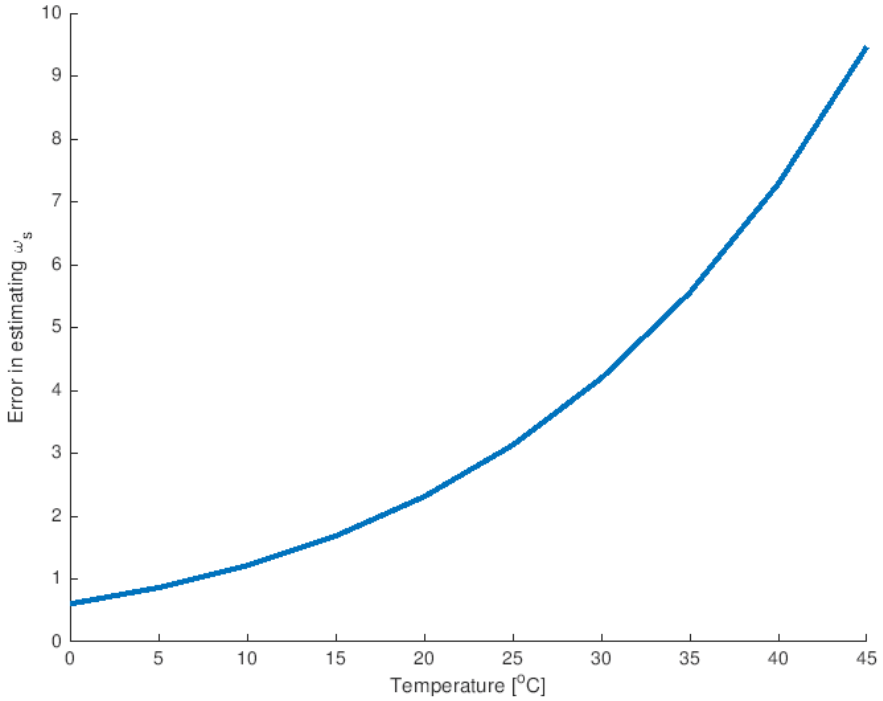

Figure 5: *Model error of the simplification in equation (2) using empirical data[8]*

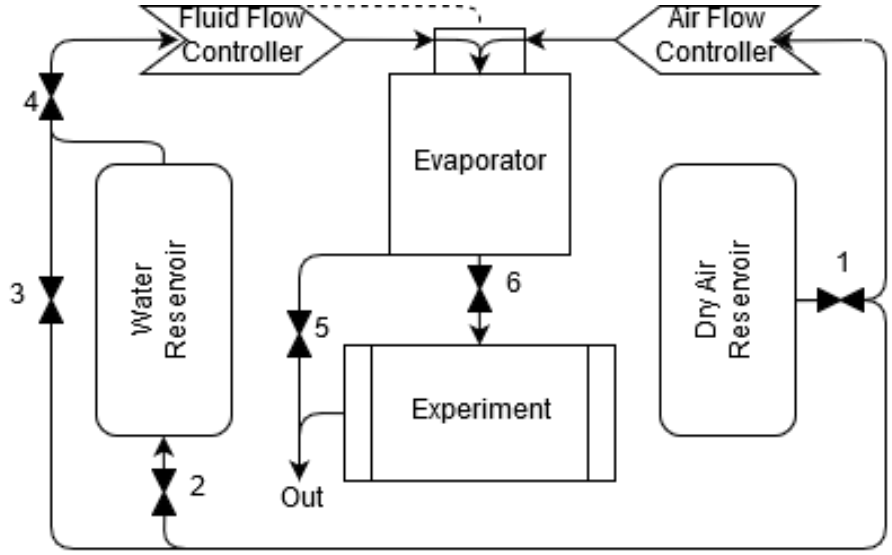

Figure 6: *Schematic overview of humidity controller and its functional elements*

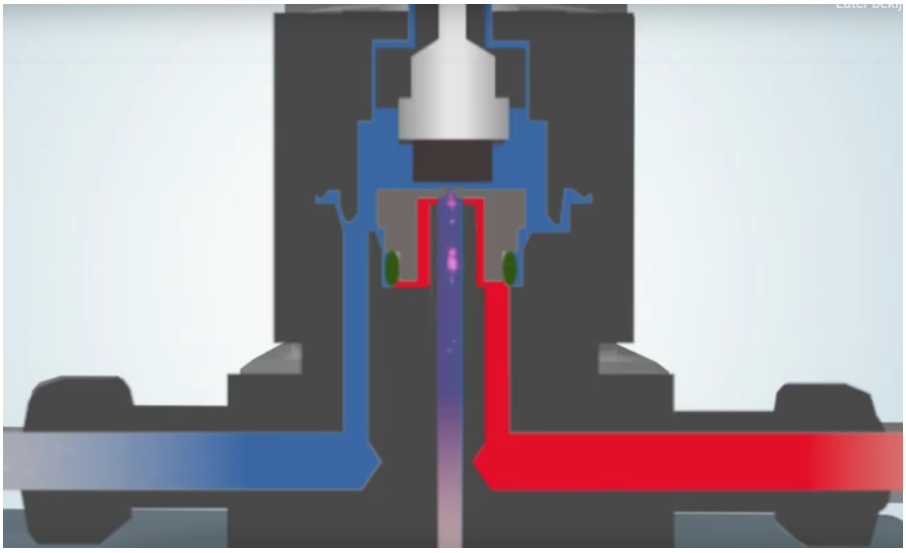

Figure 7: *Schematic diagram of the CEM mixing valve[9]*

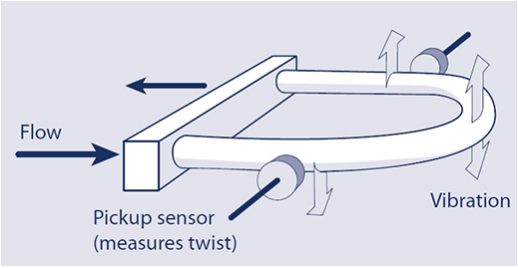

Figure 8: *Schematic diagram of the Coriolis measurement principle[12]*

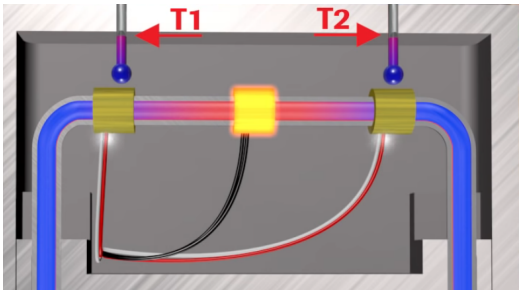

Figure 9: *Schematic diagram of temperature measurement principle[15]*

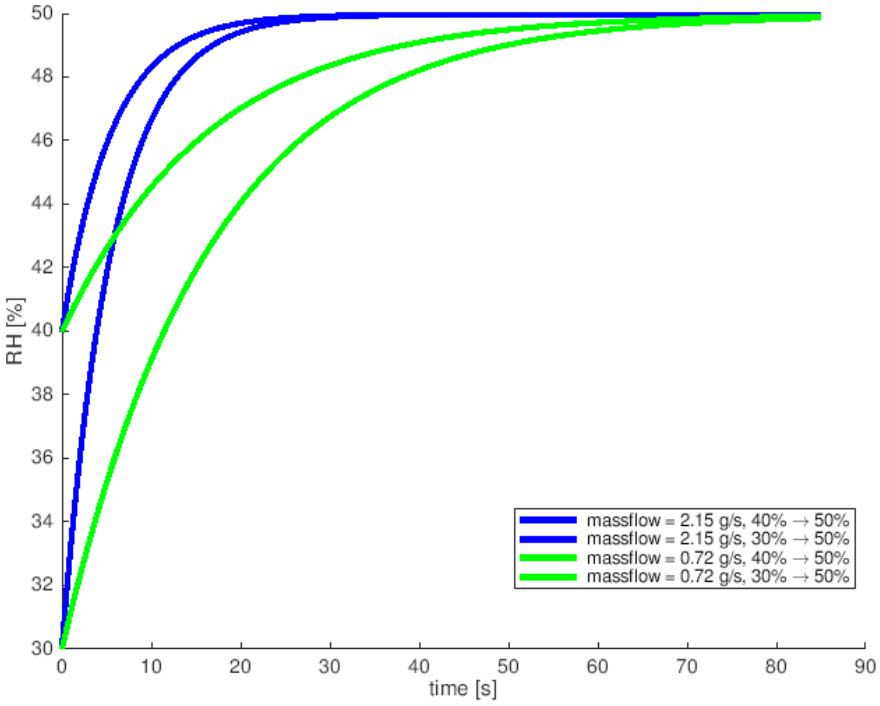

Figure 10: *Numerical results of simulating idealized system performance under maximum operating conditions*

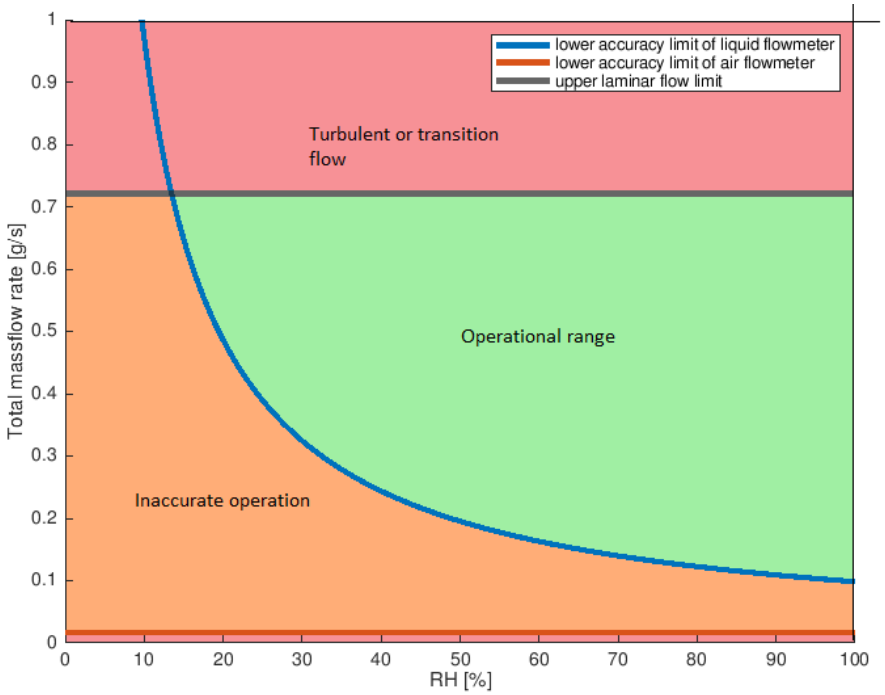

Figure 11: *Theorized operational limits of this humidifier design*